Short Papers

Wide-Bandwidth Optical Phased Array Based on Remote Coding Configuration

Amit P. Goffer, Moshe Kam, and Peter R. Herczfeld

Abstract—**Wide-bandwidth weighted array processing requires that the weighting function, applied to each element in the array, be a function of the frequency. In many applications this requirement leads to the use of costly and bulky *true-time delay* (TTD) based weighting devices. In this paper, the equivalence between a *filter embodiment* and a *correlator embodiment* of the weighting function is used to show that the *remote coding* configuration can serve as a correlation embodiment of the weighting function, thus avoiding the need for TTD's in the signal path.**

I. Background

A. Introduction

Weighted arrays (such as phased arrays for radar and communication applications) are traditionally designed with *filter embodiment* weights [1], [2]; i.e., each element of the array is implemented with an attenuator/amplifier combined with a phase-shifting device. When the communicated signal is wideband, true-time delay (TTD) based weighting devices are needed in order to avoid beam distortion and other degradations in performance [3]. However, in many applications the TTD's are bulky and costly, thus reducing the practicality of large arrays for wide-bandwidth signal processing. *Optical phased arrays* have received greater attention in recent years [4], mainly because of the promise they hold for reducing weight and volume (replacing waveguides or coaxial cables by fiber optics) for large arrays.

It is suggested here to use the equivalence of the *filter embodiment* to the *correlation embodiment* and design an array based on the remote coding configuration [6], [7], which is an efficient architecture for optically controlled microwave phased array antennas. The suggested architecture can also be implemented in microwave phased arrays (nonoptical).

B. Filter Embodiment

Let $W_m(\omega)$ be the mth weighting function ($w_m(t)$ being its inverse Fourier transform, the time-domain weighting function, as shown in Fig. 1). The output of each filter is given by the convolution

$$y_m(t) = x_m(t)^* w_m(t) = \int_{-\infty}^{\infty} x_m(\tau) w_m(t-\tau)\, d\tau. \qquad (1)$$

Because of causality, $w_m(t) = 0$ for $t < 0$. We also assume that

Manuscript received October 10, 1990; revised March 18, 1991. This work was supported by an NSF P. Y. I. Award (ECS-9057587), by GE Aerospace, by the Ben Franklin Partnership of Pennsylvania, and by the Stein Foundation.

The authors are with the Department of Electrical and Computer Engineering, Drexel University, Philadelphia, PA 19104.

IEEE Log Number 9100155.

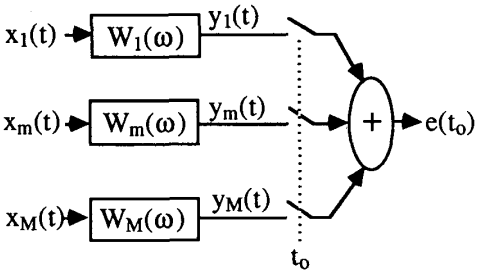

Fig. 1. Filter embodiment phased array.

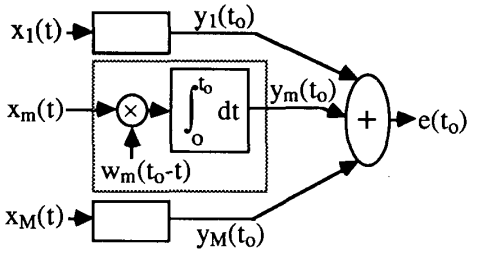

Fig. 2. Correlation embodiment phased array.

$w_m(t) = 0$ for $t > t_0$; thus in (1) $0 < t - \tau < t_0$, and

$$y_m(t) = \int_{t-t_0}^{t} x_m(\tau) w_m(t-\tau)\, d\tau. \qquad (2)$$

C. Equivalence to Correlation Embodiment

The filter embodiment configuration, can be realized as a correlation embodiment (following e.g., [5]). Inspection of (2) (with the output sampled at $t_0, y_m(t_0)$) reveals that the filter embodiment depicted in Fig. 1 is equivalent to the correlation embodiment depicted in Fig. 2. If a continuous output is required, a band-pass filter should be connected at the array output, in order to reconstruct the signal from its samples. This filter should have a passband that equals the signal bandwidth, and a center frequency that corresponds to the desired operating RF or IF. Periodic sampling in the configuration of Fig. 1 ($t_0 = nT$, $n = 0, 1, 2, \cdots$, and T the sampling interval) corresponds to applying $w_m(-t)$ periodically (i.e., applying $w_m(nT - t)$ in the configuration of Fig. 2, see also the realization in Fig. 4).

The filter embodiment realization of phased arrays (Fig. 1) represents the traditional approach, where the weights ($\{W_i(\omega)\}$) are constrained to be TTD based devices (for wide-bandwidth communication). The correlation embodiment realization studied here (Fig. 2) allows the shifting of the processing effort from the signal path (optical/microwave) to the control path ($w_m(t)$).

The correlation embodiment basically requires a double-balanced mixer (DBM) on the signal path, with the advantage of

0018-9480/91/0700-1216$01.00 ©1991 IEEE

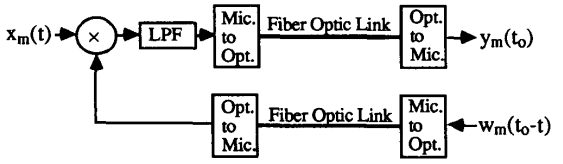

Fig. 3. Remote coding configuration. The LPF replaces the integrator of eq. (2).

low cost and small size; DBM's are available in packages smaller than the wavelength, while the size of TTD's may be several dozens of wavelengths. The insertion loss (S to Ku frequency range) is of the same order for both methods, typically 4 to 8 dB, depending on the frequency and on the number of bits (for the TTD). A nonlinearity is a disadvantage of the correlation embodiment realization; the DBM typically has a third-order intercept point of 7 to 16 dBm, while the TTD hardly introduces any intermodulation products. The operating bandwidth of the DBM is usually narrower than the TTD, but using the correlation embodiment technique, bandwidths of 50% and higher can be achieved. Another advantage of the correlation embodiment is the use of an unquantized phaser, which helps in controlling pattern side lobes and pointing resolution without increasing the volume of the hardware. The computational or weighting control complexity, as implied from Figs. 4, 6, and 7, is higher for the correlation embodiment realization.

II. Remote Coding Configuration for Wide-Band Applications

Remote coding configuration is an efficient architecture for optically controlled microwave phased array antennas [6], [7]. We adapt this configuration to the correlation embodiment weighting realization. Fig. 3 depicts the mth channel, where the low-pass filter (LPF) plays the role of an integrator (eq. (2)) and its output contains the weighted and sampled output of the mth element. The LPF output amplitude modulates a light source (a laser diode in the microwave-to-optical converter). A fiber-optic (FO) link is then used in the signal path and is terminated by a detector (in the optical-to-microwave converter). The summation over the weighted elements takes place in the microwave domain.

In the configuration of Fig. 3, the weighting is in the microwave domain, prior to the conversion to the optical domain. This configuration makes it possible to modulate the light source at a much lower rate (the bandwidth rate instead of the RF). The lower rate considerably relaxes the requirements for the light source (e.g., a light-emitting diode (LED) can be used instead of a laser diode).

III. Example: Uniform Progressive Time Delay

In many applications a wide-bandwidth uniform progressive phase is required. The mth weighting function is given by

$$W_m(\omega) = e^{-j2\pi m d u_0 f/f_0} = e^{-j\omega\tau_m} \tag{3}$$

where $\tau_m = m d u_0 / f_0$ is the time delay of the mth element, $u_0 = \sin\theta_0$, θ_0 is the pointing angle, and f_0 is the center frequency. The weighting function in the time domain is given by the inverse Fourier transform of (3): $w_m(t) = \delta(t - \tau_m)$. For instantaneous flat spectrum, nonzero at bandwidth of Δf (from $f = f_0 - \Delta f/2$ to $f = f_0 + \Delta f/2$), we have

$$w_m(t) = \int_{f_0 - \Delta f/2}^{f_0 + \Delta f/2} e^{-j\omega\tau_m} e^{j\omega t} = \frac{\sin \pi \Delta f (t - \tau_m)}{\pi (t - \tau_m)} e^{j\omega_0 (t - \tau_m)}. \tag{4}$$

If we choose our system to operate up to f_H ($= f_0 + \Delta f/2$) and allow the weighting function to be nonzero from dc to f_H, we have

$$w_m(t) = \frac{\sin \pi f_H (t - \tau_m)}{\pi (t - \tau_m)}. \tag{5}$$

Applying (4) to the configuration of Fig. 2 produces an inherent band-pass operation, which may replace a tunable RF front end. Equation (5) expresses a low-pass filtering operation, with a cutoff frequency of f_H. Therefore, two possible realizations are possible:

- Wide-bandwidth realization: the weighting system's transfer function is zero for frequencies above f_H.
- Band-pass realization: the weighting system's transfer function is a band-pass filter, with center frequency of f_0 and a bandwidth which is equal to the signal's bandwidth.

A. Wide-Bandwidth Realization

The dc to f_H weighting function (eq. (5)) is described in Fig. 4. The pulse "train" can be realized by use of a FO recirculating memory loop [8], and the weighting function generator can be realized as follows. A digitized "sinc" function is stored or produced in a computer, with the width of the "sinc" dictated by f_H; a flash D/A (digital-to-analog converter) produces the desired waveform, $w_m(t)$. The delay between waveforms can be introduced by the computer when activating the D/A's in proper timing. The flash D/A can be realized as follows (Fig. 5). The data lines which contain the sampled weighting function ("sinc") are connected to a TEM transmission line. When the switches are momentarily "on," the transmission line is charged with the desired waveform. The desired waveform propagates along the transmission line. The limiting factor to the available pulse width is the switching speed of the switches in Fig. 5. The measured speeds of p-i-n diodes are a few nanoseconds, thus restricting the operation of the weighting, f_H ($= f_0 + \Delta f/2$), to about 100 MHz. HEMT's could reach switching speeds of about 50 ps [9], allowing a frequency range up to 1 GHz. Optical switching devices may reach the picosecond range [10], allowing a frequency range up to 100 GHz.

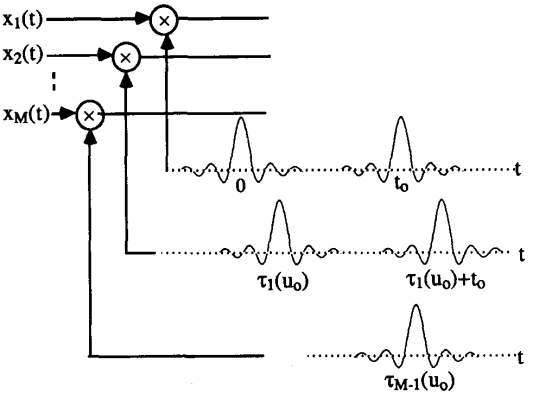

Fig. 4. Application of the weighting function of eq. (5) to the scheme of Fig. 3.

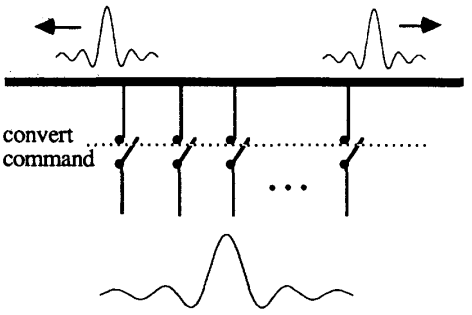

Fig. 5. Flash D/A realization.

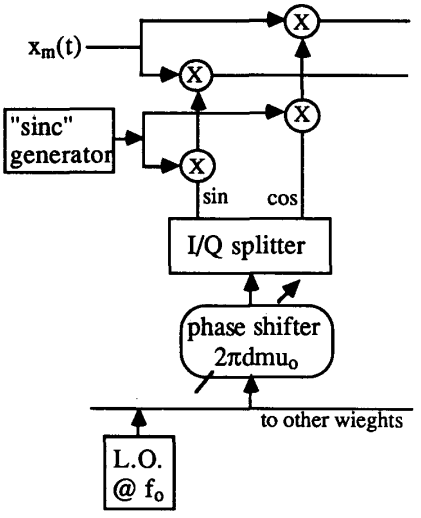

Fig. 6. Band-pass realization, with phase shifter (eq. (4)).

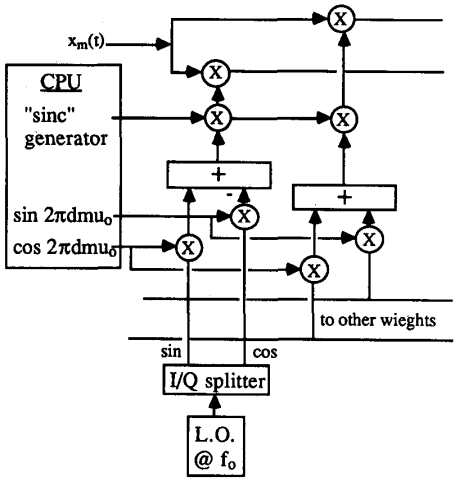

Fig. 7. Band-pass realization, without phase shifter.

B. Band-Pass Realization

When wide-bandwidth realization (eq. (5), Fig. 4) is not practical because of very high f_H, we can use the configuration stemming from (4). We note that, in contrast to the wide-bandwidth realization, the "sinc" function is much wider ($\approx 1/\Delta f$, instead of $1/f_H$); it must be multiplied by $\exp(j\omega_0 t)$ and it should be shifted by $2\pi mdu_0$ (using a *phase-shifting* device, a TTD not being necessary). The complex weighting can be realized as depicted in Fig. 6 (only the mth weighting function is illustrated) using phase shifters. The band-pass realization can also be implemented *without* phase shifters. Rewriting explicitly the exponent of (4) yields the realization shown in Fig. 7.

IV. Summary

TTD's for wide-bandwidth beam steering or shaping can be replaced by additional processing in the control path. The alternative is a correlation embodiment implemented in the remote coding configuration. The advantages of this approach are as follows:

1) Combination of correlation embodiment with the remote coding eases the selection of the light source in the FO link.
2) Elimination of the TTD from the signal path reduces the cost and size of the system.
3) The weights in the band-pass realization (Figs. 6 and 7) perform inherent (and adjustable) band-pass filtering, without additional loss and nonlinear effects.
4) Sample (and hold) operations are performed without additional circuitry.
5) The weighting functions (which include the tapering) and the operating bandwidth can be software programmable.

Three configurations were presented:

1) Wide-bandwidth realization: the weighting function operates from dc to f_H. This is the simplest configuration; however, it requires a flash D/A. The basic concept of the flash D/A was presented; it may permit operation up to 100 GHz.
2) Band-pass realization: the weighting function operates from $f = f_0 - \Delta f/2$ to $f = f_0 + \Delta f/2$. The implementation is with a phase shifter in the weighting path.
3) Band-pass realization: the implementation is without a phase shifter.

References

[1] R. J. Mailloux, "Phased array theory and technology," *Proc. IEEE*, vol. 70, pp. 246–291, Mar. 1982.
[2] A. W. Rudge, K. Milne, A. D. Oliver, and P. Knight, Eds., *The Handbook of Antenna Design*, vols. 1 and 2. London: UK: Peter Peregrinus, 1986.
[3] A. A. Oliner and G. H. Knittel, Eds., *Phased Array Antennas*. Dedham, MA: Artech House, 1972.
[4] P. R. Herczfeld, "Guest editorial," *IEEE Trans. Microwave Theory Tech.*, vol. 38, pp. 465–466, May 1990.
[5] H. Urkowitz, *Signal Theory and Random Processes*. Dedham, MA: Artech House, 1983.
[6] P. R. Herczfeld and A. S. Daryoush, "Recent developments related to an optically-controlled microwave phased array antenna," in *SPIE '88* (Boston), Sept. 1988.
[7] I. Koffman *et al.*, "Comparison of various architectures of microwave fiber-optic links: A system level analysis," in *SPIE Proc. Fiber Optic Systems for Mobile Platforms* (San Diego), Aug. 1987.

[8] I. Koffman, P. R. Herczfeld, and A. S. Daryoush, "A fiber optic recirculating memory loop for radar applications," *Microwave and Opt. Technol. Lett.*, vol. 1, no. 9, Sept. 1988.
[9] R. N. Simon and K. B. Bhasin, "Analysis of optically controlled microwave/millimeter wave device structures," in *1986 MTT-S Int. Microwave Symp. Dig.*, June 1986, pp. 551–554.
[10] C. H. Lee, "Picoseconds optics and microwave technology," *IEEE Trans. Microwave Theory Tech.*, vol. 38, pp. 596–607, May 1990.

Higher Order Mode Coupling Effects in the Feeding Waveguide of a Planar Slot Array

Sembiam R. Rengarajan

Abstract—**Method of moments solutions to pertinent coupled integral equations have been investigated for arrays of coupling slots of the centered-inclined and longitudinal-transverse types between a main waveguide and crossed branch waveguides. It has been demonstrated that, by including the TE_{20} mode coupling in the analysis, most of the higher order mode effects can be accounted for in reduced height waveguides, whereas in waveguides of standard height there may be a small additional effect arising from the TE_{01} mode coupling.**

I. Introduction

Recently, two types of resonant coupling slots commonly employed in waveguide-fed planar slot arrays have been analyzed [1]–[3]. The scattering wave representations and equivalent circuit models of slots are based on the TE_{10} mode scattering off the slot. In the main waveguide, higher order mode coupling, especially through the TE_{20} mode, between adjacent coupling slots can introduce a small but significant error in the slot aperture electric field, which in turn gives rise to errors in the TE_{10} mode scattering in the two waveguides. Such errors can affect a high-performance slot array by degrading the side lobe level or input match. Previously, the internal higher order mode coupling between *radiating* slots has been considered in the design of a slot array [4]. The objective of this paper is to investigate the effect of internal higher order modes in the feeding waveguide of a planar slot array. Both the centered-inclined coupling slot and the longitudinal-transverse coupling slot have been considered.

II. Method of Analysis

Fig. 1(a) shows a main waveguide and three crossed branch waveguides on top. Centered coupling slots are cut in the common broad walls between the main and branch waveguides. Fig. 1(b) illustrates a similar arrangement with longitudinal-transverse coupling slots. It is assumed that all the branch waveguide ends are terminated by matched loads and that they do not have any radiating slots. The main waveguide is fed by a matched TE_{10} mode source at one end and match terminated at the other end. By enforcing the continuity of the longitudinal component of the magnetic field across six apertures of thick walled slots, we obtain six coupled integral equations in terms of the transverse component of the aperture E fields [1], [3], [6]–[8]. The integral equations have been solved by the global Galerkin type method of moments, resulting in matrix equations expressed in the form

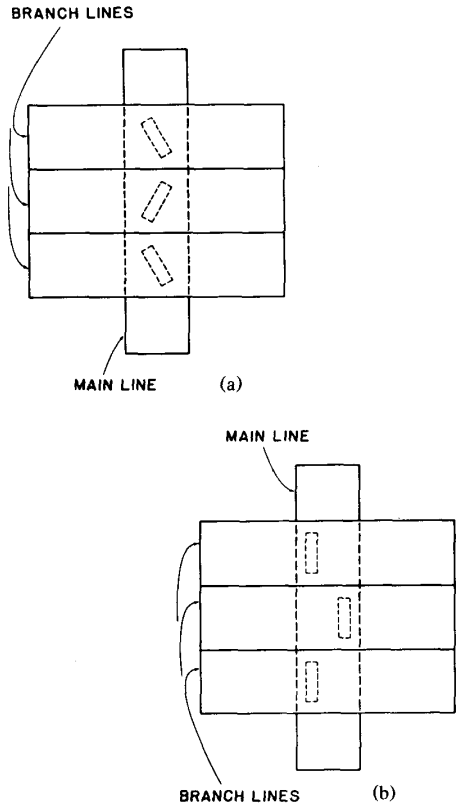

Fig. 1. (a) Centered-inclined coupling slots feeding three branch waveguides. (b) Longitudinal-transverse coupling slots feeding three branch waveguides.

$$\begin{bmatrix} [Y_{11}] & [Y_{12}] & [G^{12}] & [0] & [G^{13}] & [0] \\ [Y_{21}] & [Y_{22}] & [0] & [0] & [0] & [0] \\ [G^{21}] & [0] & [Y'_{11}] & [Y'_{12}] & [G^{23}] & [0] \\ [0] & [0] & [Y'_{21}] & [Y'_{22}] & [0] & [0] \\ [G^{31}] & [0] & [G^{32}] & [0] & [Y''_{11}] & [Y''_{12}] \\ [0] & [0] & [0] & [0] & [Y''_{21}] & [Y''_{22}] \end{bmatrix} \begin{bmatrix} \underline{A}_1 \\ \underline{A}'_1 \\ \underline{A}_2 \\ \underline{A}'_2 \\ \underline{A}_3 \\ \underline{A}'_3 \end{bmatrix} = \begin{bmatrix} \underline{I}_1 \\ \underline{0} \\ \underline{I}_2 \\ \underline{0} \\ \underline{I}_3 \\ \underline{0} \end{bmatrix} \quad (1)$$

Manuscript received March 21, 1990; revised February 27, 1991. This work was supported by the Hughes Aircraft Company, by the University of California, Los Angeles, and by California State University, Northridge.

The author is with the Department of Electrical and Computer Engineering, California State University, Northridge, CA 91330.

IEEE Log Number 9100150.

0018-9480/91/0700-1219$01.00 ©1991 IEEE